RSC Advances

ROYAL SOCIETY OF CHEMISTRY

www.rsc.org/advances

RSC Advances

RSCPublishing

PAPER

Reaction time effect of straw-like MoO_3 prepared with a facile, additive-free hydrothermal process

Cite this: DOI: 10.1039/x0xx00000x

Y.L. Yang, Y. Shen,* and Z. Li

(Faculty of Material Science and Chemistry, China University of Geosciences, Wuhan, Wuhan 430074, China. Zhejiang Research Institute, China University of Geosciences, Wuhan, Hangzhou 310000, China.)

Received 00th January 2014,
Accepted 00th January 2014

DOI: 10.1039/x0xx00000x

www.rsc.org/

Production of molybdenum oxide materials with novel morphology exhibiting unique functions is challenging. Here we investigate the growth process of molybdenum oxide powder with straw-like structures via a facile and additive-free hydrothermal process by varying the reaction time. The crystal structure, morphology and microstructure of samples were characterized to understand the mechanism of formation. Furthermore, optical properties were characterized by ultraviolet-visible diffuse reflectance spectroscopy and color difference meter. The results demonstrate that the as-prepared MoO_3 powders possess the same absorption threshold 420 nm and band gap of 3.16 eV. In addition, we found that the nanofibers were peeled off from the prisms and the median state of the product (columnar structures with cavities surrounded by nanofibers) exhibits the most optimal photochromic properties due to the enhanced light harvesting from multiple light reflections and scattering in-between the cavities of the MoO_3 columnar structures.

1. Introduction

Transition-metal oxides can have attractive photochromic properties[1] resulting from band-gap excitation and have potential applications in areas of information display, sensors and high-density memory devices.[2-10] Among various transition-metal oxides, molybdenum trioxide (MoO_3) as one of the well-known n-type semiconductors[3] is attractive due to its various applications in many fields. Additionally, photochromic MoO_3 presents possible applications in optical storage systems, display devices, and smart windows due to its great apparent coloration efficiency under light excitation.[11] Therefore, photochromic MoO_3 is attracting increasing attention.

To date, MoO_3 materials with improved optical properties can be achieved by modulating their microstructures and morphologies.[12-14] Morphologies of MoO_3 materials are found to be important factors that affect the sensing of the excitation light source.[15] Multi-hole structures, generally with plentiful cavities, could enhance light harvesting from multiple light reflections and scattering in-between the cavities. For this reason, the utilization efficiency of exciting light can be improved.[16] Hence, it is worthwhile to synthesize molybdenum oxide materials with novel morphologies especially multi-hole structures. Generally, MoO_3 with neat hexagonal prisms could be easily obtained via hydrothermal rout. Recently, Yi Shen[17,18] and Deki[19] successfully synthesized MoO_3 hexagonal prisms by hydrothermal method. However, the photochromic performance of MoO_3 with neat hexagonal prisms was poor. Besides, Phuruangrat[20] reported MoO_3 nanofibers with 50 nm in diameter and 10-12 nm in length were produced by hydrothermal reaction. As the crystal sizes of MoO_3 decrease dramatically and the nanofibers always go with large exposed surface area,[21,22] the performance of sample is obviously improved. According to our previous research,[23-25] we found that the morphologies of MoO_3 in our experiment usually present to be prisms and fibers. As research continues, we find a phenomenon that all fibers are transformed from the prisms. What's more, there are no reports of this phenomenon so far. Interestingly, the median state (columnar structures with cavities surrounded by nanofibers) of the transformation process reveals better performance than prisms and fibers. It is noticed that the formation process of the unique median state is extremely complicated. In addition, this special structure can be modulated only during a specific period in a precise regulation process.

In this work, hexagonal MoO_3 powders were synthesized by a facile, additive-free hydrothermal method with different reaction times. The influences of hydrothermal reaction times on morphologies and photochromic properties of MoO_3 powders were also investigated. Moreover, the possible growth process was intensively discussed in this paper.

2. Experimental

2.1. Preparation of the molybdenum oxide powders

All chemicals were of analytical grade purity and used as received without purification. The pure water was obtained from a Milli-Q synthesis system. In a typical procedure, the sodium molybdenum powder was dissolved by distilled water to a concentration of 0.08 M, and the $Na_2MoO_4 \cdot 2H_2O$ solution was acidified to a fixed pH of 1.0 by concentrated HCl solution (37-38 wt%). After being stirred for 240 min, as-prepared precursor was transferred into the 100 ml Teflon-lined stainless steel autoclave. Then the autoclave was sealed and maintained at 120 °C for 3 h, 6 h, 9 h, 12 h, 24 h, 48 h and 72 h, respectively. Finally, the product was collected and washed

sequentially with water and ethanol, then finally dried at 60 °C in the vacuum.

2.2. Characterization

The crystal structure informations of the resulting products were analyzed by X-ray diffraction (XRD, D8-FOCUS, Bruker AXS) with a Cu-K_α radiation source (λ = 0.1541 nm) and settings of 40 mA and 40 kV at a scanning rate of 0.01° per 0.05 s in the 2θ range from 5° to 75°. The surface morphologies were characterized by scanning electron microscopy (SEM, JSM-5610LV, Japan, 20KV) and transmission electron microscopy (TEM, 100SX Rigaku, Japan). The texture properties of MoO_3 powders were determined by multi-point BET nitrogen adsorption (ASAP2020, Micromeritics). Furthermore, photochromic properties of the resulting products were tested by ultraviolet-visible diffuse reflectance spectroscopy (UV-vis, Shimadzu UV-2550, Japan) with $BaSO_4$ as the baseline correction, combined with color difference meter.[26]

3. Results and discussion

3.1. Phase analysis

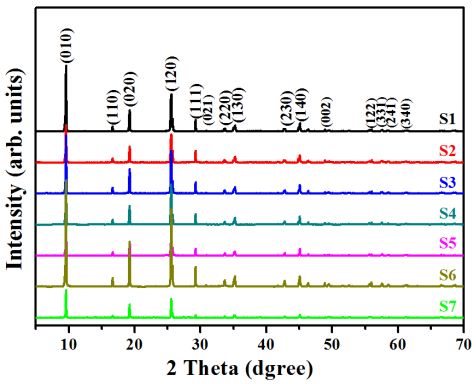

Fig 1. XRD patterns of the products obtained after different hydrothermal reaction times at 120 °C: S1 3 h, S2 6 h, S3 9 h, S4 12 h, S5 24 h, S6 48 h and S7 72 h.

Fig. 1 shows the X-ray diffraction patterns of products prepared at 120 °C with different reaction times. The XRD patterns clearly show that all the diffraction peaks of the products can be indexed to the hexagonal structure of MoO_3 (PDF Card no. 48-0399) with a space group P 6_3/m (176). No other impurities were detected in the final products. The results indicate that hydrothermal reaction time has no obvious effects on the crystalline phase of MoO_3 products.

3.2. Microstructure investigations

The time-dependent morphology of the sample is demonstrated in Figs 2 and 3. Fig. 2a shows that when the reaction time is 3 h, the product consists of neat hexagonal prisms with widths of 7-10 μm and lengths of 25-40 μm. When the reaction time is elongated to 6 h, lots of tiny rifts appear on the exterior of the prisms. Meanwhile, the edges of the prisms even begin to crack (shown in Fig. 2b). With the reaction time beyond 9 h (Fig. 2c), a small quantity of nanofibers are formed around the prisms with the edges of the prisms tending to be fuzzy. With the dwelling time increases to 12 h, plentiful nanofibers almost cover the whole surface of the prisms and the edge of the prism has partly disappeared (shown in Fig. 2d). This process continues until all the edges disappear. The image in Fig. 3e reveals that the shape of prisms is broken and many nanofibers come off from the prisms after reacting for 24 h. Closer observation demonstrates that the complete hexagonal prisms eventually grow into columnar structures with cavities. However, when the reaction time increasing to 48 h the surfaces of the fragmentary prisms (columnar structure with plentiful cavities) are gathered with extensive nanofibers and the clear-cut columnar structures are still absent (its corresponding SEM image is shown in Fig. 3f). After reacting for 72 h (Fig. 3g), the columnar structures disappear entirely and change into a straw-like structure. Obviously, hydrothermal reaction time has a great impact on the morphologies of MoO_3.

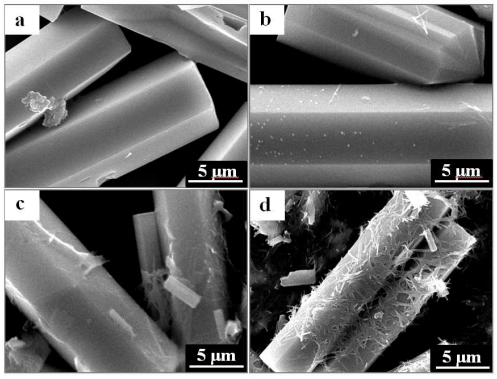

Fig 2. SEM images of MoO_3 synthesized with different hydrothermal reaction times at 120 °C: (a) 3 h, (b) 6 h, (c) 9 h and (d) 12 h.

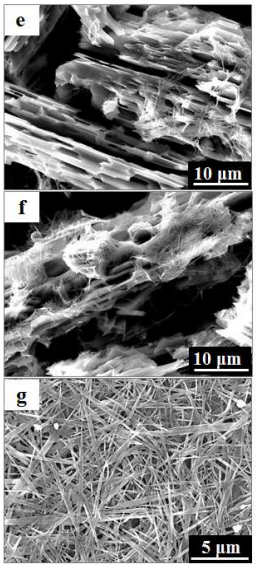

Fig 3. SEM images of MoO_3 synthesized with different reaction times: (e) 24 h, (f) 48 h and (g) 72 h.

The microstructures of the as-prepared MoO_3 products with different reaction times were further investigated by TEM, and the results were shown in Fig 4. Shown in Fig. 4a is a TEM image taken from the sample after hydrothermal reaction for 12 h. The assembled nanofibers and smaller prisms (no obvious cavities on the surface) could be clearly seen, in accordance with SEM results in Fig. 2d. When prolonging the reaction time to 24 and 48 h, the solid prism-like structures are broken. Obvious strip-like cavities could be observed in Fig. 4 (b-c). In addition, the microstructures of the final structures are thin which could be verified by the light-colored part in the vision of TEM images. Fig. 4d displays that plenty of nanofibers were synthesized after reacting for 72 h and these nanofibers gathered together closely. Apparently, there are no prisms with strip-like cavities in Fig. 4d. According to the results of SAED

patterns (shown in the insets of Fig. 4), the samples are hexagonal and well-crystallized, consistent with the XRD analysis.

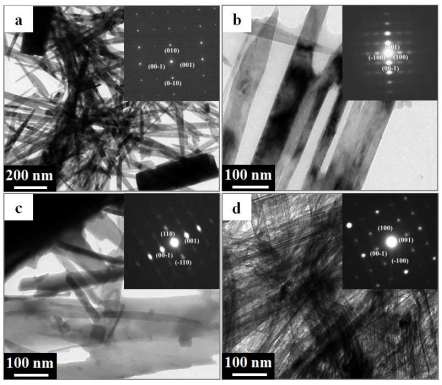

Fig 4. TEM images and SAED (selected-area electron diffraction) patterns of MoO_3 powders: (a) sample S4; (b) sample S5; (c) sample 6; (d) sample S7.

According to the above experimental results, a plausible growth mechanism of the straw-like structure is illustrated in Scheme 1. The formation process of MoO_3 powder could be described into the reaction equations below:

$MoO_4^{2-} + H^+ = HMoO_4^-$ (1)

$HMoO_4^- + H^+ = H_2MoO_4$ (aq) (2)

H_2MoO_4 (aq) = $MoO_3 \cdot H_2O$ (3)

In the initial reaction period, the pH of the solution increases with increasing temperature to 120 °C, causing increased formation of H_2MoO_4 and more MoO_3 will be acquired.[27] Moreover, the neat hexagonal prisms are formed readily and rapidly driven by the inherent symmetry in hexagonal system[28] and the crystallization of MoO_3 tends to be saturated. Subsequently, the MoO_3 crystal will begin to dissolve into the intermediate species (H_2MoO_4) on account of the hydrothermal acidic system with high pressure. In the hydrothermal system with 120 °C, the dissolution process is certainly gentle and tardy. As the molybdic acid is hard to dissolve in water,[29] the newly generated H_2MoO_4 may immediately change into MoO_3 under holding temperature at 120 °C. In fact, the crystal growth of MoO_3 is a delicate balance between the circulating dissolution and recrystallization process of MoO_3. There are only a few MoO_3 dissolving each time owing to the limited reaction conditions, then the tiny recrystallized MoO_3 has no enough concentration to aggregate and grow into a large grain. Massive tiny recrystallized MoO_3 might be generated immediately along with the large MoO_3 grain gradually dissolving in the solution. Finally, the distribution of recrystallized MoO_3 becomes unordered. It is worth mentioning that the recrystallized MoO_3 also possess hexagonal structure according to the SAED result in insets of Fig 4(b-d).

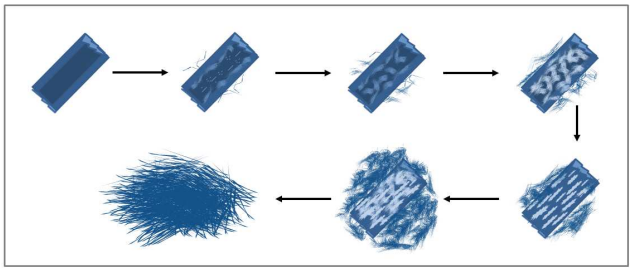

Scheme 1. Schematic illustration of the formation process of straw-like MoO_3.

When the reaction duration proceeded to a certain value, the as-formed hexagonal prisms experienced a gradual morphological evolution of nanofiber growth. Note that the initiation of nanofibers starts from the edge of the prisms (the energy of the edge is higher),[30] followed by the spot cracking of the prismatic planes (Fig. 2b and c). As the reaction proceeding, the nanofibers continue coming off from the prisms and gather together around the hexagonal prism. The formation of more and more nanofibers leads to the corresponding cavities left over on the hexagonal prism. After reacting long enough, all the hexagonal prisms disappear and change into straw-like structures. This formation mechanism is supported by the microstructural evolution process of the material as a function of the reaction duration (Fig. 2 a-d, Fig. 3 e-g).

3.3. The texture properties of all MoO_3 products

The BET surface area, pore volume and average pore size were summarized in Table 1. The results of their BET surface area, pore volume and pore size are tabulated in Table 1. It can be concluded that as the hexagonal prisms change into straw-like structures, the surface area and pore volume of the MoO_3 powder both reveal an increasing tendency. However, the maximum value reached at the median state (S6).

Table. 1 Textural properties of MoO_3 powder prepared on different conditions.

Sample	S1	S2	S3	S4	S5	S6	S7
BET surface area ($m^2 \cdot g^{-1}$)	0.0015	0.0027	0.0424	0.1704	7.523	7.968	3.569
Pore volume ($cm^3 \cdot g^{-1}$)	0.000815	0.000937	0.001096	0.005097	0.0176	0.0192	0.00615
Pore size (nm)	-	-	-	-	10.194	10.286	2.452

3.4. Photochromic phenomenon

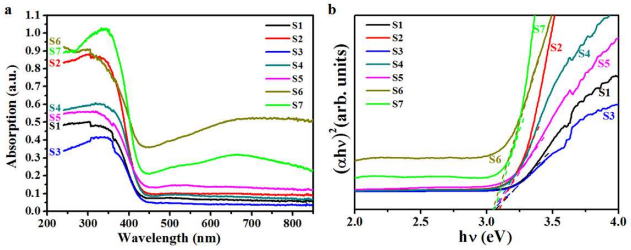

Fig 5. (a) UV-vis diffuses reflectance spectra of MoO_3 with different reaction times; (b) Plot of $(\alpha h\upsilon)^2$ versus photon energy of MoO_3 powders synthesized with different reaction times.

As all samples are non-transparent, the as-prepared powders are apparently opaque to the light. Then the light cannot be transmitted through the powders whether they can adsorb light. Therefore, the adsorption spectra rather than transmission spectra of samples are used to characterize the optical properties. The UV-vis diffuses reflectance spectrum of MoO_3 powders with different reaction times in the wavelength range from 280 to 850 nm is shown in Fig. 5(a). As S6 exhibits wider adsorption wavelength range in Fig. 5(a), it is guessed that S6 may reveal better photochromic sensibility under the same light source. The observed absorption threshold around 420 nm is due to the intrinsic absorption at the semiconductor band gap.[31] A minor change in the absorption thresholds of all samples was observed as the reaction time increased. Thus, we can assume that the reaction time has no significant impact on the band gap. The direct band gap (E_g) was calculated from the relation between the absorption coefficient and photon energy given by

$\alpha h\upsilon = (h\upsilon - E_g)^n$ (4)

where α, h, υ and E_g are the absorbance, Planck constant, photon frequency, and photonic band gap, respectively. The parameter n is a constant associated with the different types of electronic transition: n = 1/2, 2, 3/2 or 3 for direct allowed, indirect allowed, direct forbidden and indirect forbidden transitions, respectively.[32-34] Fig. 5(b) shows the plot of $(\alpha h\upsilon)^2$ vs $h\upsilon$. By extrapolating the linear portion of the curve to zero absorbance, the direct E_g of MoO_3 powders were determined to be 3.16 eV in good agreement with the reported values.[35]

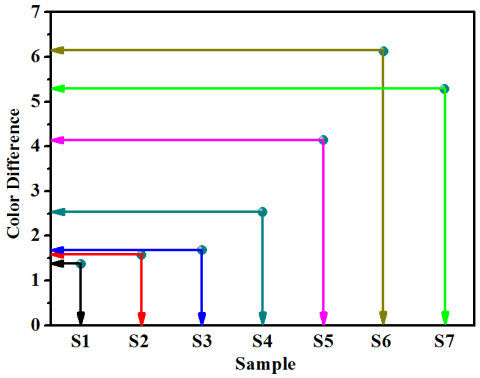

Fig 6. Plot of color difference with different reaction times of all products.

Irradiated by 3W ultraviolet lamp, the MoO_3 powders synthesized with various reaction times were tested by color difference meter. The plot of color difference values is demonstrated in Fig 6. It is obviously observed that the color difference of samples increase with the reaction time. Among them, samples S1, S2 and S3 increase slightly while samples S4 and S5 show a higher growth range. Obviously, sample S6 prepared with a reaction time of 48 h possesses the maximum color difference value, indicating its better photochromic property.

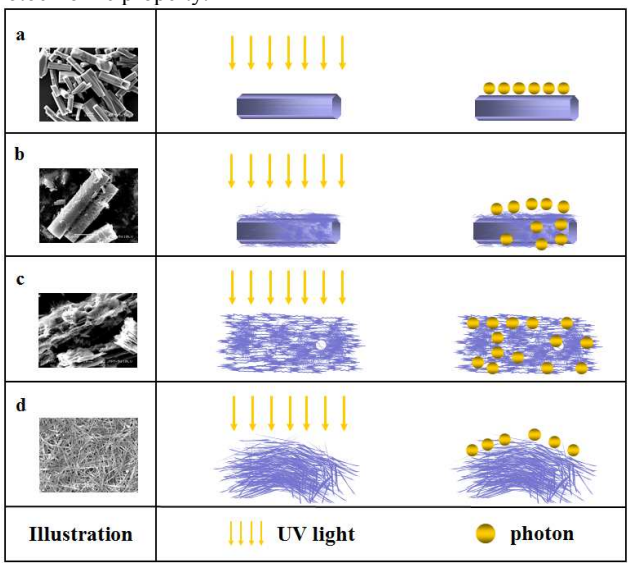

Fig 7. Schematic illustrations of four different morphologies of MoO_3 powders exposed in the UV light: (a) neat hexagonal prisms; (b) hexagonal prisms with nanofibers (c) columnar structures with cavities surrounded by nanofibers; (d) straw-like structures.

Fig. 7 is the schematic illustration of four different MoO_3 powders exposed in the UV light. It is shown that MoO_3 powders prepared with different reaction times respectively consist of neat hexagonal prisms (3 h, Fig. 7a), hexagonal prisms with nanofibers (reacting for 6 h and 9 h, Fig. 7b), columnar structures with cavities surrounded by nanofibers (holding for 12 h, 24 h and 48 h, Fig. 7c), and closely packed straw-like structures (72 h, Fig. 7d). Apparently, the columnar structures with cavities surrounded by nanofibers (Fig. 7c) possess more loose structures in comparison to other structures. These multi-hole structures could provide a larger exposed surface area (Table. 1), which is of great benefit to absorption of excitation light, thus resulting in increase of protons and photo-generated electron-hole pairs.[36] In addition, the utilization efficiency of exciting light can be improved due to the enhanced light harvesting from multiple light reflections and scattering in-between the cavities of the MoO_3 columnar structures.[16] According to the model of double insertion-extraction of ions and electrons,[37] the high number of protons and photo-generated electron-hole pairs has a beneficial effect on the photochromic properties of the powders.[22,35] Therefore, the sample obtained by reacting for 48 h got the optimized photochromic property, attributed to the columnar structures with cavities surrounded by nanofibers. On the contrary, neat hexagonal prismatic structures, hexagonal prisms with nanofibers and fallen straw-like structures possessing less exposed surface area result in a smaller quantity of protons and photo-generated electron-hole pairs. Then, the corresponding photochromic properties of S6 are superior to other samples.

4. Conclusions

In summary, we have demonstrated the fabrication of MoO_3 powder with straw-like structures, based on a facile, additive-free hydrothermal process. Time-dependent investigations reveal a multi-step growth mechanism. The variety of reaction time has a great impact on the final product morphology. According to the experimental results, the final product with straw-like structures growing from neat hexagonal prisms attribute to nanofibers constantly come off from the prisms with the increase of the hydrothermal reaction time. In this process, the sample obtained with the hydrothermal reaction time of 48 h exhibits the optimized photochromic performance due to the columnar structures with cavities surrounded by nanofibers possessing larger exposed surface area.

Acknowledgements

This work was supported by the National Natural Science Foundation of China (grant no. 51102087).

References

1 R. J. Colton, A. M. Guzman, J. W. Rabalais, Acc. Chem. Res., 1978, 11, 170-176.
2 Y. A. Yang, Y. W. Cao, B. H. Loo, J. N. Yao, J. Phys. Chem. B, 1998, 102, 9392-9396.
3 A. Khademi, R. Azimirad, A. A. Zavarian, A. Z. Moshfegh, J. Phys. Chem. C, 2009, 113, 19298-19304.
4 J. N. Yao, K. Hashimoto, A. Fujishima, Nature 1992, 355, 624-626.
5 M. D. Giulio, D. Manno, G. Micocci, A. Serra, A. Tepore, Phys. Status Solidi A, 1998, 168, 249-256.
6 M. Ferroni, V. Guidi, G. Martinelli, M. Sacerdoti, P. Nelli, G. Sberveglieri, Sens. Actuators B, 1998, 48, 285-288.
7 D. Manno, M. D. Giulio, A. Serra, T. Siciliano, G. Micocci, J. Phys. D, 2002, 35, 228-231.
8 C. Imawan, H. Steffes, F. Solzbacher, E. Obermeier, Sens.

Actuators B, 2001, 77, 346-351.
9 M. E. Harlin, L. B. Backman, A. O. I. Krause, O. J. T. Jylha, J. Catal., 1999, 183, 300-313.
10 H. Liu, E. Iglesia, J. Catal., 2002, 208, 1-5.
11 L. Zheng, Y. Xu, D. Jin, Y. Xie, Chem. Mater., 2009, 21, 5681-5690.
12 F. Xu, Y. N. Lu, Y. Xie, Y. F. Liu, Mater. Des., 2009, 30, 1704-1711.
13 J. Polleux, N. Pinna, M. Antonietti, M. Niederberger, J. Am. Chem. Soc., 2005, 127, 15595-15601.
14 J. G. Yu, X. X. Yu, B. B. Huang, X. Y. Zhang, Y. Dai, Cryst. Growth Des., 2009, 3, 1474-1480.
15 V. Nirupama, K. R. Gunasekhar, B. Sreedhar, S. Uthanna, Curr. Appl. Phys., 2010, 10, 272-278.
16 X.Y. Lai, J.E. Halpert, D. Wang, Energy Environ. Sci., 2012, 5, 5604-5618.
17 Y. Shen, Y. L. Xiao, P. Yan, Y. L. Yang, F. P. Hu, Z. Li, J. Alloys Compd., 2014, 588, 676-680.
18 Y. Shen, F. P. Hu, Y. L. Yang, Y. L. Xiao, P. Yan, Z. Li, Surf. Coat. Technol., 2014, 240, 393-398.
19 S. Deki, A. B. Béléké, Y. Kotani, M. Mizuhata, J. Solid State Chem., 2009, 182, 2362-2367.
20 A. Phuruangrat, D. J. Ham, S. Thongtem, J. S. Lee, Electrochem. Commun., 2009, 11, 1740-1743.
21 F. Zhang, Q. Wu, X. B. Wang, N. Liu, J. Yang, Y. M. Hu, L. S. Yu, X. Z. Wang, Z. Hu, J. M. Zhu, J. Phys Chem. C, 2009, 113, 4053-4058.
22 R. C. Xie, J. K. Shang, J. Mater. Sci., 2007, 42, 6583-6589.
23 Y. Shen, Y. L. Yang, F. P. Hu, Y. L. Xiao, P. Yan, Z. Li, Mater. Sci. Semicond. Process., 2014, http: //dx.doi.org/10.1016/j. mssp.2014.03.055
24 Y. Shen, R. Huang, Y. Li, S. Z. Yao, Appl. Surf. Sci., 2011, 258, 414-418.
25 M. Y. Yan, Y. Shen, L. Zhao, Z. Li, Mater. Res. Bull., 2011, 46, 1648-1653.
26 P. Meduri, E. Clark, J. H. Kim, E. Dayalan, G. U. Sumanasekera, M. K. Sunkara, Nano Lett., 2012, 12, 1784-1788.
27 K. U. Rempel, A. E. Williams-Jones, A. A. Migdisov, Geochim. Cosmochim. Acta, 2009, 73, 3381-3392.
28 Y. Shen, D. F. Ding, Y. L. Yang, Z. Li, L. Zhao, Mater. Res. Bull., 2013, 48, 2317-2324.
29 M. Takami, Copper foil for printed circuit board, United State Patent No. 4619871.
30 K. Byrappa, M. Yoshimura, William Andrew Publishing, USA, New York, 2001.
31 P. Singh, A. Kumar, Deepak, D. Kaur, J. Cryst. Growth, 2007, 306, 303-310.
32 Y. Keereeta, T. Thongtem, S. Thongtem, J. Alloys Compd., 2011, 509, 6689-6695.
33 T. Thongtem, S. Jattukul, Ch. Pilapong, S. Thongtem, Curr. Appl. Phys., 2012, 12, 23-30.
34 S. Suwanboon, R. Tanattha, R. Tanakorn, Songklanakarin, J. Sci. Technol., 2008, 30, 65-69.
35 B. L. Mordike, T. Ebert, Mater. Sci. Eng. A, 2001, 302, 37-45.
36 P. Badica, Cryst. Growth Des., 2007, 7, 794-801.
37 Y. Shen, D. F. Ding, Y. Z. Deng, Powder Technol., 2011, 211, 114-119.

Reaction time effect of straw-like MoO_3 prepared with a facile, additive-free hydrothermal process

Y.L. Yang, Y. Shen,* and Z. Li

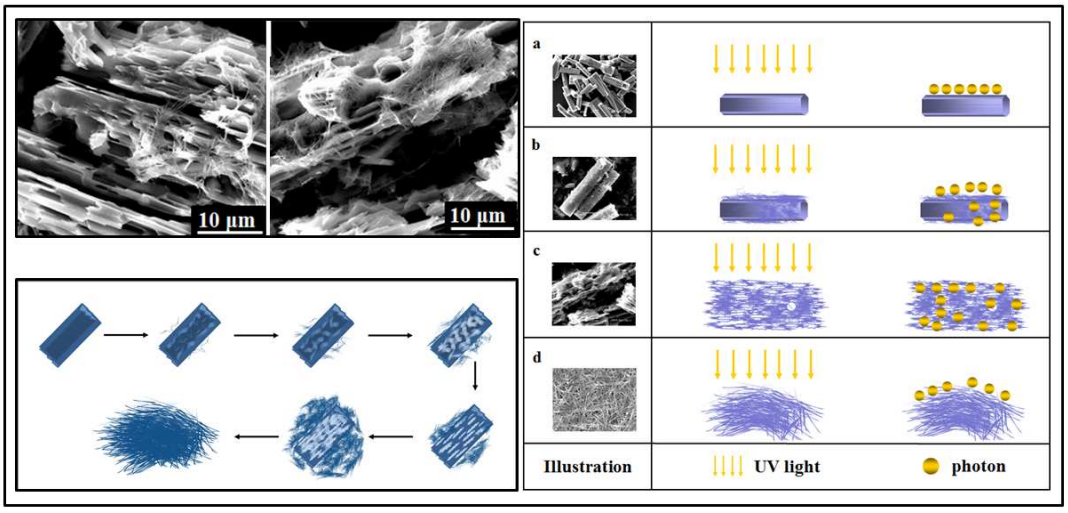

This paper presents the synthesis of straw-like MoO_3 prepared with a facile, additive-free hydrothermal process. The effects of reaction times on morphologies and properties of MoO_3 have been investigated. In addition, a plausible growth mechanism of the straw-like structure is illustrated according to the experimental results. It is worth mentioning that the median state of the product (columnar structures with cavities surrounded by nanofibers) exhibits the most optimal photochromic properties. The result may own to strip-like cavities of the columnar MoO_3 hierarchical nanostructures with enhanced light harvesting from multiple light reflections and scattering in-between the cavities.